NASA-CR-202086

EMAT Inspection of Space Shuttle External Tank Welds

R. Polen
Martin Marietta Manned Space Systems
New Orleans, LA 70189
(504) 257-1828

P. Latimer
Babcock & Wilcox
P.O. Box 11165
Lynchburg, VA 24506
(804) 522-6154

W. Latham
Babcock & Wilcox
P.O. Box 11165
Lynchburg, VA 24506
(804) 522-5765

D. MacLauchlan
Babcock & Wilcox
P.O. Box 11165
Lynchburg, VA 24506
(804) 522-5765

R. Neuschaefer
NASA
Marshall Space Flight Center
Huntsville, AL
(205) 544-7382

Introduction – Technology developed by Babcock & Wilcox for use on the Advanced Solid Rocket Motor has led NASA's External Tank (ET) project office and Martin Marietta Manned Space Systems to contract Babcock & Wilcox Research & Development Division to evaluate the use of electromagnetic acoustical transducer (EMAT) technology as a replacement for penetrant and X-ray weld inspection on the ET. The feasibility task performed and the development of prototype systems are described in this paper.

Technical Considerations – EMATs are particularly useful for weld examination because no couplant is needed, thus allowing rapid scanning at ambient or elevated temperatures. It is desirable to scan without a raster motion (motion toward and away from the weld) to cover the full weld geometry from the root to the crown. If the weld region is flooded with sound, the scan of the weld can be linear and greatly simplify the mechanical fixturing. The problem with this approach is that the root and crown signal are so prominent that they interfere with the flaw signals. Babcock & Wilcox has developed a technique that will eliminate the root and crown signals in a linear weld scan. This technique uses a collinear set of focused EMAT sensors rotated at an angle to the weld center line. The frequency is chosen so that the wavelength is comparable to the flaw dimensions. As a result, the flaw can be detected by diffraction over a wide range of angles.

The Experimental Technique – The experimental technique is illustrated in Figure 1. Two collinear focused EMATs are rotated at a suitable angle to the weld centerline. In practice, the angle can be any convenient value if the wavelength of the sound is sufficiently close to the flaw dimensions that the flaw acts as a point source and thus exhibits a wide angular diffraction pattern. This technique has the advantage that the angle can be easily changed. Theoretical diffraction curves were generated as a model in the selection of angles and the wavelength/flaw dimension ratio. The computer program for the model was based upon Huygens' principle since the results must be valid in the near field as well as the far field. A typical diffraction pattern based on this model is shown in Figure 2.

The EMAT Sensors – In order to increase the signal to noise ratio for small flaws using the diffraction technique, focused sensors were used for both surface breaking and volumetric flaws. The focus is a point for surface breaking flaws and a line for vertically polarized shear waves (SV). The coils are pitch-catch with the surface wave coil having a focal length of 1.5". For SV waves the separation of the conductors was twice that used for the surface waves sensor, and the focal length was 1 5/8". Both types of sensors had a frequency of 1.95 MHz. The sensor coil was a flexible printed circuit using one ounce copper on 0.002" kapton. The sensor coil was covered with a two mil protective layer of kapton. The normal magnetic field was supplied by a stack of two neodymium iron boron magnets. The sensors and feasibility fixture are shown Figure 3. The two surface wave sensors are oriented at $\pm 45°$ with respect to the weld center line. The SV wave sensor is also oriented at an angle of 34° with the weld center line. This sensor arrangement is required for complete coverage of one side of the weld. The arrangement of sensors for the prototype system is shown in Figure 4. The production system will have a similar set of sensors on both sides of the weld bead.

The Calibration Plates and Instrumentation – The primary calibration plate was of 2219 Aluminum (Al) with dimensions of 5' x 7' and contained a tungsten inert gas (TIG) weld. This panel contains electrodischarge machined (EDM) notches on both OD and ID surfaces in both the weld bead and heat affected zone (HAZ). A total of 24 EDM slots 0.050" long by 0.025" deep by 0.004" wide were installed in the weld crown, root, and parent metal to check flaw detection and coverage. The EDM notches were oriented perpendicular to the weld, parallel to the weld, and ±45° to the weld axis. This panel also had a series of through drilled holes ranging from 0.020" to 0.100" diameter and two 0.047" diameter through-drilled holes spaced 0.240"apart (edge to edge) to check system sensitivity, resolution, and repeatability. Three tapered, Al 2219 standards contained slots in the range of 0.030" to 0.20" length. Additional panels containing buried flaws and induced cracks were also examined. A computer interface module allowed the system to be programmed via a serial communications link. Each channel was capable of operating at a different frequency, gain, magnet pulse length, etc. from the other channels.

Experimental Results – The two wave modes that were used were 32° SV waves and surface waves. The 32° beam angle for the SV mode is fixed as a result of the shape of the directivity curve for this wave mode. The primary panel was scanned using two 2 MHz surface wave sensors oriented at ± 45° with respect to the weld axis. This technique located all surface breaking flaws that were located on one side of the weld line on the same side of the panel as the sensor. It was necessary to have two sensors orthogonal to each other in order to detect any flaws parallel to any one sensor. The results indicate that all surface breaking flaws are detected on the root side by this technique. Similar results were obtained for the crown side of the panel. The holes in the primary panel were scanned with a 1.95 MHz line focused SV wave angle beam EMAT. All through holes were detected by this technique including the smallest size with a 0.020" diameter. In addition, the 0.047" diameter through hole pairs were resolved as two distinct indications.

The Plasma Welded Panels – Plasma welded panels were also evaluated as a comparison with the TIG welded primary sample. These samples contained tapered welds and the inspection capability was demonstrated with the 1.95 MHz line focused SV wave. The root of the TIG welded primary panel is much smoother than the plasma root; therefore, it was necessary to establish feasibility on both types of welds. A typical result obtained from a scan of the plasma welded sample is shown in Figure 5. These panels also contained flaw lengths in the range of 0.030" to 0.200". The results of the scans indicated that all flaw sizes in that range could be detected. The excellent signal to noise ratio from the 30 mil flaw is illustrated in Figure 6.

Induced Cracks and Buried Flaws – EMAT techniques were evaluated with actual cracks as well as EDM notches. Feasibility was demonstrated with a panel that contained a series of induced cracks. The cracks were detected with excellent signal to noise ratio (Figure 7) using 2 MHz EMAT surface waves throughout the weld. Several samples containing typical buried flaws such as porosity and lack of fusion were examined with the line focused SV wave EMAT. The results indicated that buried flaws could be detected with an efficiency comparable to conventional ultrasonic techniques. A typical result is shown in Figure 8 where an area with lack of fusion is detected in both root and crown scans.

Conclusions – The results of the feasibility testing and evaluation during prototype development show that EMATs have the potential to provide a cost effective and highly reliable alternative to penetrant and selected X-ray inspections on the ET. Babcock & Wilcox's technology advancement on EMATs and support from the NDE and Quality personnel of the Marshall Space Flight ET Program Office have contributed to the excellent results on this project.

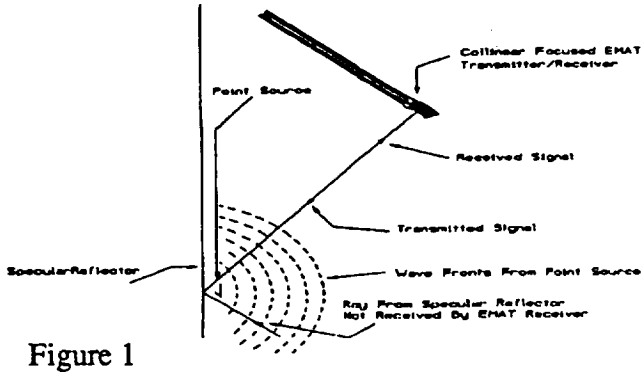

Figure 1

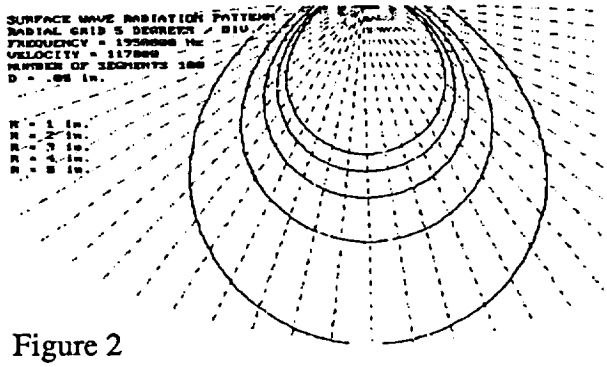

Figure 2

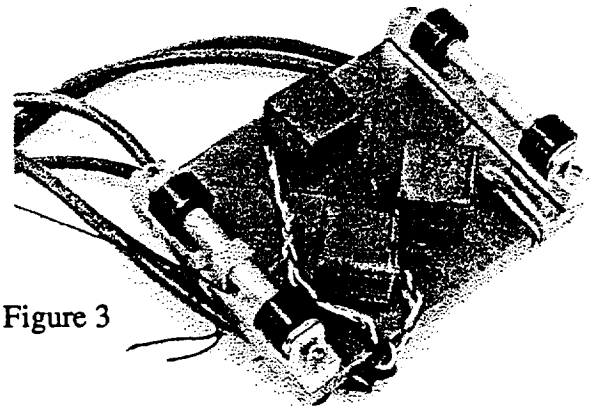

Figure 3

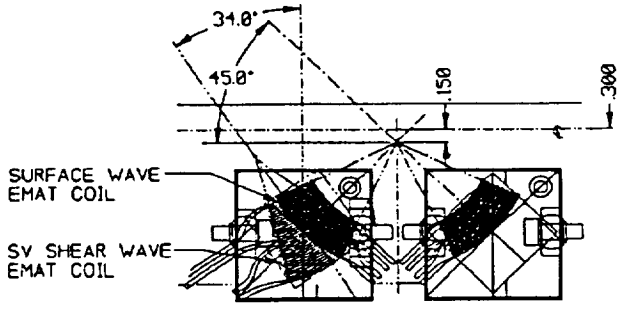

Figure 4

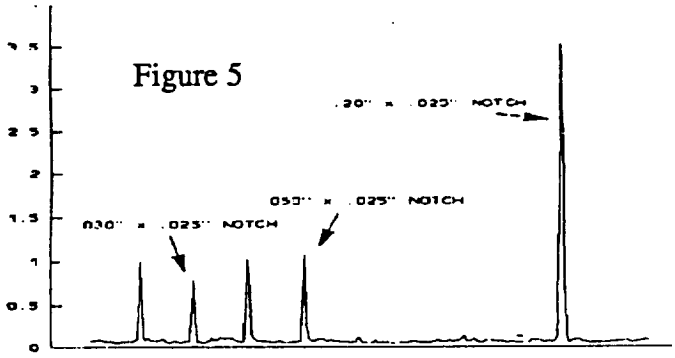

Figure 5

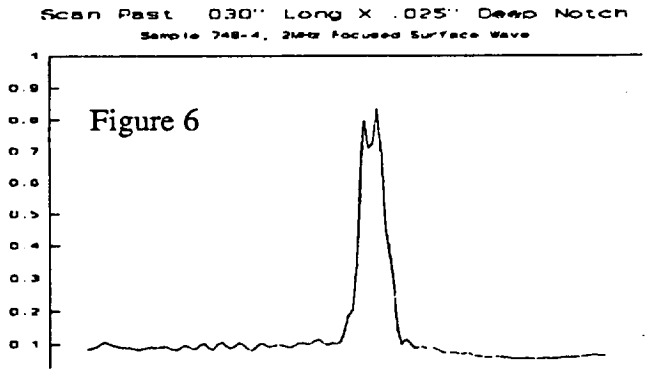

Figure 6

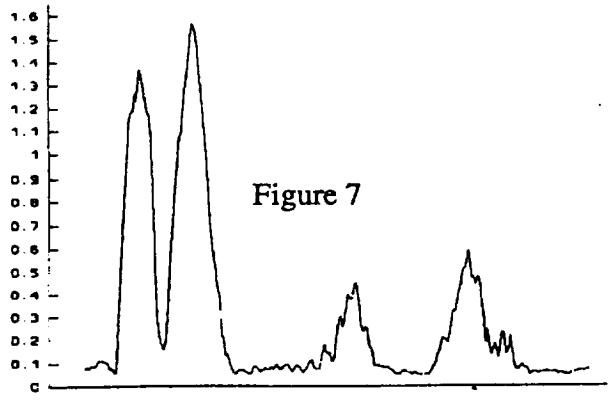

Figure 7

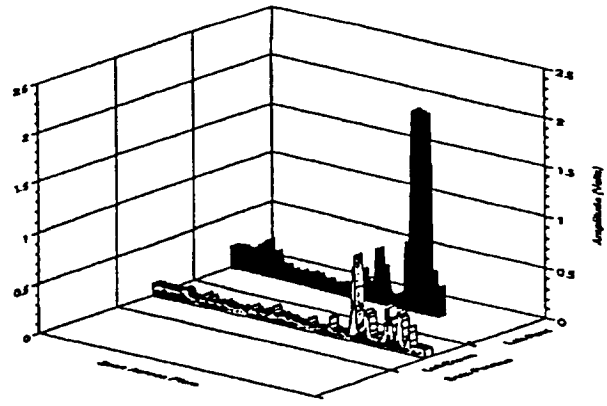

Figure 8